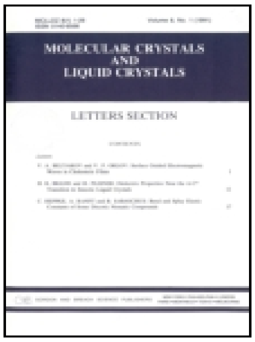

Taylor & Francis
Taylor & Francis Group

Molecular Crystals and Liquid Crystals

ISSN: 1542-1406 (Print) 1563-5287 (Online) Journal homepage: http://www.tandfonline.com/loi/gmcl20

Synthesis, Characterization, Crystal Structure, and Hirshfeld Surface Analysis of 2–(2–Hydroxy–3–methoxyphenyl)–1–(4–methylphenyl)–4, 5–diphenyl–1H–imidazole

M. Prabhuswamy, S. Viveka, M. M. M. Abdoh, K. J. Pampa, G. K. Nagaraja & N. K. Lokanath

To cite this article: M. Prabhuswamy, S. Viveka, M. M. M. Abdoh, K. J. Pampa, G. K. Nagaraja & N. K. Lokanath (2015) Synthesis, Characterization, Crystal Structure, and Hirshfeld Surface Analysis of 2–(2–Hydroxy–3–methoxyphenyl)–1–(4–methylphenyl)–4, 5–diphenyl–1H–imidazole, Molecular Crystals and Liquid Crystals, 616:1, 226-236, DOI: 10.1080/15421406.2014.991139

To link to this article: http://dx.doi.org/10.1080/15421406.2014.991139

Mol. Cryst. Liq. Cryst., Vol. 616: pp. 226–236, 2015
Copyright © Taylor & Francis Group, LLC
ISSN: 1542-1406 print/1563-5287 online
DOI: 10.1080/15421406.2014.991139

Synthesis, Characterization, Crystal Structure, and Hirshfeld Surface Analysis of 2–(2–Hydroxy–3–methoxyphenyl)–1–(4–methylphenyl)–4,5–diphenyl–1*H*–imidazole

M. PRABHUSWAMY,[1] S. VIVEKA,[2] M. M. M. ABDOH,[3]
K. J. PAMPA,[4] G. K. NAGARAJA,[2] AND N. K. LOKANATH[1,*]

[1]Department of Studies in Physics, University of Mysore, Mysore, Karnataka, India
[2]Department of Chemistry, Mangalore University, Mangalore, Karnataka, India
[3]Faculty of Science, Department of Physics, An Najah National University, Nabtus West Bank, Palestinian Territories
[4]Department of Studies in Microbiology, University of Mysore, Mysore, Karnataka, India

The substituted imidazole $C_{29}H_{24}N_2O_2$ was prepared via multicomponent reactions and the product crystallized using dimethylformamide. The structure of the compound was established by elemental analysis, FT-IR, thermogravimetric analysis, UV-Visible, and single-crystal X-ray diffraction. The molecule is crystallized in the tetragonal crystal system with the space group $P4_32_12$ and with unit cell parameters $a = 12.226(1)$ Å, $b = 12.226(1)$ Å, $c = 31.807(3)$ Å, *and* $Z = 8$. *The molecular and crystal structure of the title molecule is stabilized by intramolecular interactions, O—H···N and C—H···N, and intermolecular interaction, C—H···O.*

Keywords Crystallization; crystal structure; FTIR spectrum; hirshfeld surface; imidazole; intermolecular interactions; multicomponent reaction; thermo gram

1. Introduction

Heterocycles are the largest classical divisions of organic chemistry and are of immense importance biologically as well as in industrially. For more than a century, heterocycles have constituted one of the largest areas of research in organic chemistry. The presence of heterocycles in all kinds of organic compounds of interest in electronics, biology, optics, pharmacology, material sciences, and so on is very well known.

Over the century, imidazole derivatives have received significant attention due to their reactions and biochemical properties. The imidazole ring system is one of the most

---

[*] Address correspondence to N. K. Lokanath, Department of Studies in Physics, University of Mysore, Mysore, Karnataka 570 006, India. E-mail: lokanath@physics.uni-mysore.ac.in

Color versions of one or more of the figures in the article can be found online at www.tandfonline.com/gmcl.

important substructures found in a large number of natural products, and biologically active compounds like amino acid histidine, the hypnotic agent etomidate [1], the proton pump inhibitor omeprazole [2], the fungicide ketoconazole [3], and the benzodiazepine antagonist flumazenil are imidazole derivatives. Highly substituted imidazoles like lepidilines A and B [4] exhibit micromolar cytotoxicity against several human cancer cell lines. The imidazole compounds are also used in photography as photosensitive compound [5]. Imidazole has varying applications in industries and extensively as a corrosion inhibitor on certain transition metals, such as copper. The thermostable polybenzimidazole (PBI) contains imidazole fused to a benzene ring and linked to benzene, and acts as a fire retardant. Apart from these imidazole is a part of the theophylline molecule, found in tea leaves and coffee beans, which stimulates the central nervous system. Because of their great importance, many synthetic strategies have been developed. In 1882, Radziszewski and Japp reported the first synthesis of the imidazole from 1,2-dicarbonyl compound, used various aldehydes and ammonia, to obtain the 2,4,5-triphenyl imidazoles [6]. In 1980, Breslow discovered that the Diels-Alder reaction performed in water could be subjected to huge rate accelerations [7]. Crystal structure of the similar imidazole derivatives, 2,4,5-triphenyl [8] and 1,2,4,5-tetraphenyl imidazole [9–10] are reported. In view of the above observations, we synthesized the title compound via four-component condensation of a benzil with substituted benzaldehyde, aniline, and ammonium acetate. Here we report the synthesis of 2–(2–Hydroxy–3–methoxyphenyl)–1–(4–methylphenyl)–4, 5–diphenyl–1*H*–imidazole, and it's characterization by the single-crystal X-ray diffraction, ^{1}H NMR, FT-IR, Thermogravimetric analysis (TGA), UV-Visible Spectra, and elemental analysis.

2. Experimental

2.1. Materials and Methods

All chemicals were purchased commercially and used without prior purification. Infrared spectra was recorded on a Shimadzu FT-IR spectrophotometer in the range 400–4000 cm^{-1} using the KBr pellets. A TA-SQT Q600 thermogravimetric analyzer was used to obtain TGA curve under nitrogen atmosphere with a heating rate of 20°C min^{-1}. The UV-Vis spectrum was recorded in Shimadzu UV-2550 UV-Visible spectrophotometer. Elemental analysis was carried out by using VARIO EL-III (Elementar 10 Analysensysteme GmBH), and melting point was determined in open capillary tube and uncorrected.

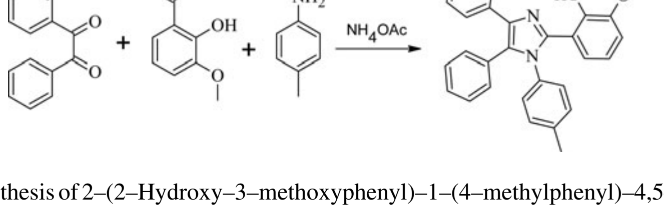

Scheme 1. Synthesis of 2–(2–Hydroxy–3–methoxyphenyl)–1–(4–methylphenyl)–4,5–diphenyl–1H–imidazol

Table 1. Elemental analysis for $C_{29}H_{24}N_2O_2$

Element	Experimental (%)	Calculated (%)
Carbon	80.58	80.53
Nitrogen	6.55	6.48
Hydrogen	5.57	5.59

2.2. Synthesis of the Compound 2–(2–Hydroxy–3–methoxyphenyl)–1–(4–methylphenyl)–4,5–diphenyl–1H–imidazole

Benzil (10 mmol), ortho vanillin (10 mmol), *p*-Toluidine (10 mmol), and ammonium acetate (12 mmol) were dissolved in boiling glacial acetic acid and refluxed for 6–8 h. The reaction progress was monitored by thin layer chromatography. After the completion of the reaction, the reaction mixture was poured into ice-water, the obtained compound was recrystallized from dimethylformamide. The product shown in Scheme 1 was obtained as white crystals which yield 83% and m.p. 163°C–166°C.

3. Results and Discussion

3.1. Elemental Analysis

In order to confirm the chemical composition of the synthesized compound Carbon (C), Hydrogen (H), and Nitrogen (N), analysis was carried out. The experimental and calculated percentages of C, H, and N are given in Table 1. The differences between experimental and calculated percentages of C, H, and N were very close to each other and within the experimental errors. This confirms the formation of the product in the stoichiometries proportion.

3.2. UV-Vis Spectral Analysis

The UV-vis spectrum of the compound is shown in Fig. 1. The UV-Visible (UV-Vis) absorption spectra of the title compound were recorded in a methanol solvent.

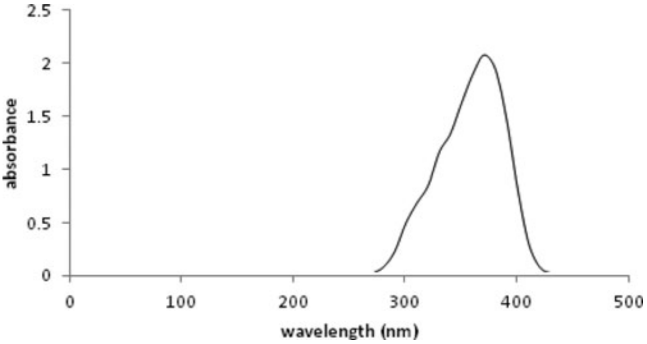

Figure 1. UV-visible spectrum of the crystal.

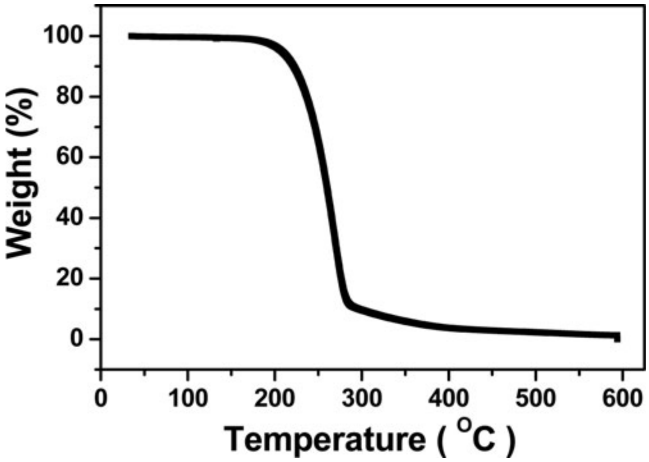

Figure 2. TGA curve of crystal.

From the graph, it was observed that the compound shows an absorption peak at 368 nm.

3.3. *Thermal Gravimetric Analysis (TGA)*

The compound decomposes mainly in one stage on heating between 200°C to 300°C as shown in Fig. 2.

There was no much weight loss observed around 140°C and shows the absence of moisture in the crystal. A higher weight loss of around 90% occurs within 200°C to 280°C. Above 300°C, 10% of the residue was left out which was due to the charring of carbon.

3.4. *FT-IR Spectral Analysis*

The FT-IR spectrum of the crystal structure is shown in Fig. 3. The board band at 3161 cm^{-1} corresponds to the O—H stretching vibration modes. The C—H stretching mode is superimposed in 2794 cm^{-1}. The 1633 cm^{-1} and 1600 cm^{-1} was due to C=N and C=C stretching, respectively. The peaks observed at 1215 cm^{-1} and 1082 cm^{-1} are due to C-O stretching vibration, 1388 cm^{-1} assigned for the aromatic amines (C-N). The above-mentioned functional group is in well agreement with the title compound.

3.5. *Single-crystal X-ray Diffraction Method*

A white block-shaped single crystal of dimension 0.17 × 0.21 × 0.23 mm of the title compound was selected for the data collection. X-ray intensity data were collected for the title compound at temperature 296 K using Bruker X8 Proteum2 X-ray diffractometer [11] with X-ray generator operating at 45 kV and 10 mA (CuK_α radiation of wavelength $\lambda = 1.54178$ Å). Data were collected with different settings of ϕ (0° and 90°), keeping the scan width of 0.5°, exposure time of 5 s, and the sample to detector distance was set to 45.10 mm. A complete data set was processed using *SAINT PLUS* [12]. The structure was solved by direct methods and refined by full-matrix least squares method on F^2 using *SHELXS* and

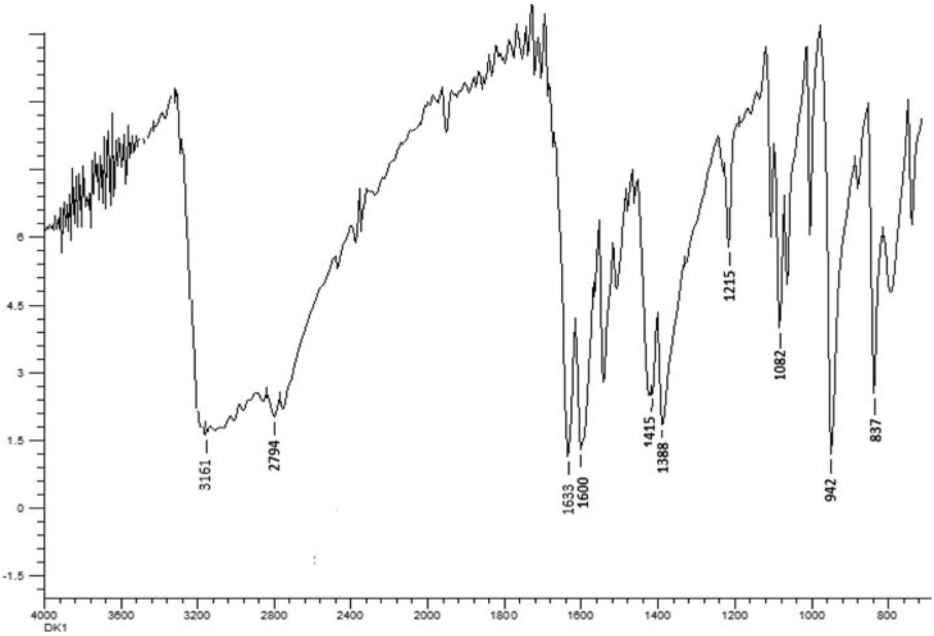

Figure 3. FTIR spectrum of the crystal.

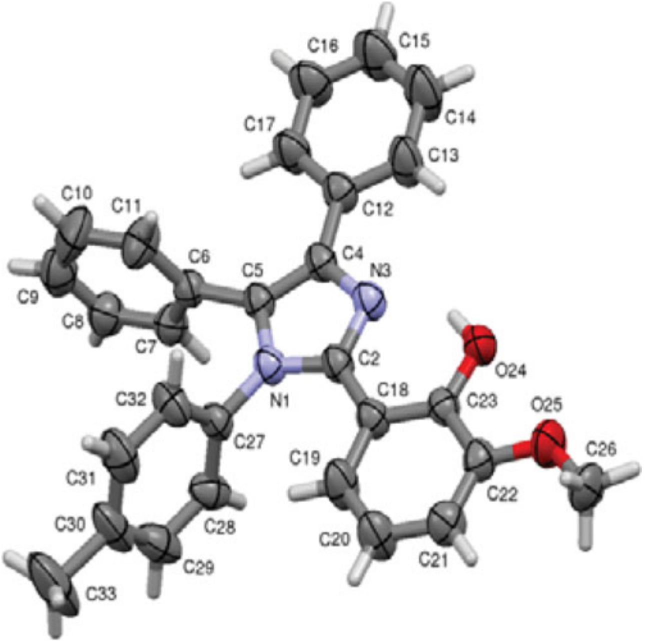

Figure 4. *ORTEP* of the molecule with numbering scheme for non-hydrogen atoms at 30% probability level.

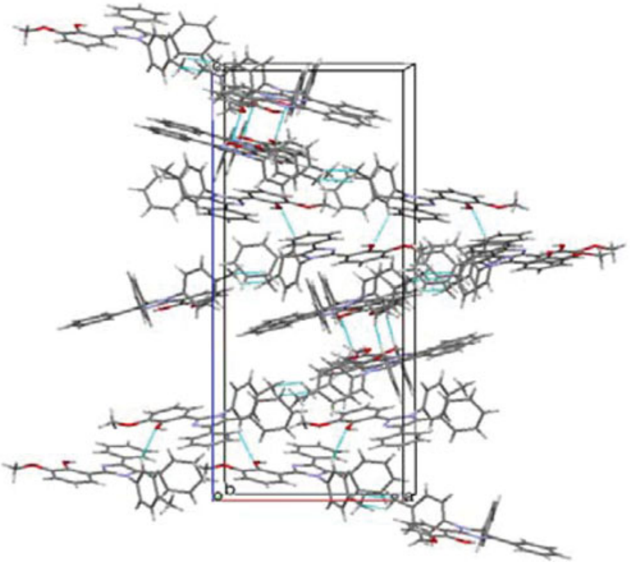

Figure 5. Packing of the molecules when viewed down along *b* axis. The dotted lines represent C—H···O hydrogen bond interactions.

SHELXL [13]. All the nonhydrogen atoms were revealed in the first difference Fourier map itself. After several cycles of refinement, the final difference Fourier map showed peaks of no chemical significance and the residual is saturated to 0.046. The geometrical calculations were carried out using *PLATON* [14]. The molecular and packing diagrams were generated using the software *MERCURY* [15].

X-ray diffraction analysis revealed that the title compound is crystallized in the tetragonal crystal system with the space group $P4_32_12$ and with unit cell parameters $a = 12.226(1)$ Å, $b = 12.226(1)$ Å, $c = 31.807(3)$ Å, and $V = 4754.5(7)$ Å^3. The *ORTEP* of the molecule with displacement ellipsoids drawn at 30% probability level is shown in Fig. 4.

Packing of the molecules when viewed down along *b* axis is shown in Fig. 5. The crystal data and the details of the structure refinement are given in Table 2. Bond lengths and bond angles are given in Table 3 and Table 4 lists the torsion angles.

The bond lengths and bond angles of the title compound are comparable with those reported earlier imidazole derivative, Lophine (2,4,5–Triphenyl–1*H*–imidazole) [16]. The imidazole ring N1/C2/N3/C4/C5 is planar as confirmed by the torsion angles of its segments. Torsion angles of 170.5(3)° for the segment O25–C26 about C26–O25–C22–C23 and 179.4(3)° for the segment C23–O24 about O24–C23–C22–C21 reflects that the methoxy and hydroxy groups are in an +*Anti-Periplanar* conformation with respect to the plane defined by the phenyl ring C18/C19/C20/C21/C22/C23.

The planes described by the phenyl ring C6/C7/C8/C9/C10/C11 and methylphenyl ring C27/C28/C29/C30/C31/C32 form dihedral angles of 89.7(2)° and 85.4(2)°, respectively, showing that they lie in equatorial positions with respect to the plane described by the imidazole ring N1/C2/N3/C4/C5. The dihedral angles of 1.3(2)° and 2.0(2)° formed, respectively, by the plane of the phenyl ring C12/C13/C14/C15/C16/C17 and the plane of the methoxyphenol ring C18/C19/C20/C21/C22/C23 reflects that they lie in axial positions with reference to the plane defined by the imidazole ring.

Table 2. Crystal data and details of structure refinement

CCDC Number	CCDC 973661
Empirical formula	$C_{29}H_{24}N_2O_2$
Formula weight	432.5 g mol^{-1}
Temperature	296 K
Wavelength	1.54178 Å
Crystal system, space group	Tetragonal, $P4_32_12$
Unit cell dimensions	$a = 12.226(1)$ Å $b = 12.226(1)$ Å $c = 31.807(3)$ Å
Volume	4754.5(7) $Å^3$
Z, Calculated density	8, 1.208 Mg/m^3
Absorption coefficient	0.602 mm^{-1}
F_{000}	1824
Crystal size	0.17 × 0.21 × 0.23 mm
Theta ranges for data collection	3.9 to 64.7°
Limiting indices	$-14 \le h \le 10, -14 \le k \le 13, -35 \le l \le 24$
Reflections collected / unique	17137 / 3915 ($R_{int} = 0.039$)
Absorption correction	multi-scan, $T_{min} = 0.874$ and $T_{max} = 0.904$
Refinement method	Full-matrix least-squares on F^2
Data/restraints/parameters	3915/0/300
Goodness-of-fit on $F2$	1.03
Final R indices [I>2sigma(I)]	$R1 = 0.046$, $wR2 = 0.107$
R indices (all data)	$R1 = 0.080$, $wR2 = 0.127$
Largest diff. peak and hole	0.12 and −0.13 e. $Å^{-3}$

The molecules exhibit C—H···*Cg* interaction; C7—H7···Cg_4 (Cg_4 is the centroid of the ring C18/C19/C20/C21/C22/C23) with a C—*Cg* distance of 3.640(3) Å, H—*Cg* distance of 2.76 Å, C—H···*Cg* angle of 158°, and with a symmetry code 1/2+x, 1/2−y, 1/4−z. The molecules also exhibit intramolecular interactions, C—H···N and O—H···N forming

Table 3. Selected bond lengths and bond angles (°)

O24—C23	1.346(3)	N1—C27	1.433(3)
O25—C22	1.362(3)	N1—C2	1.373(3)
O25—C26	1.413(4)	N3—C4	1.381(3)
N1—C5	1.381(3)	N3—C2	1.328(3)
C22—O25—C26	118.7(3)	N3—C4—C5	108.7(2)
C2—N1—C5	107.6(2)	N1—C5—C6	119.8(2)
C2—N1—C27	129.6(2)	N1—C5—C4	106.7(2)
C5—N1—C27	122.9(2)	O25—C22—C21	124.1(3)
C2—N3—C4	107.6(2)	O25—C22—C23	115.2(3)
N1—C2—N3	109.5(2)	O24—C23—C22	117.0(2)
N3—C2—C18	123.0(2)	O24—C23—C18	123.0(2)
N1—C2—C18	127.5(2)	N1—C27—C32	118.9(3)
N3—C4—C12	120.9(2)	N1—C27—C28	119.9(3)

Table 4. Torsion angles (°)

C26—O25—C22—C23	170.5(3)	C5—C6—C11—C10	−177.9(3)
C26—O25—C22—C21	−10.0(5)	C6—C7—C8—C9	−0.9(5)
C5—N1—C2—C18	−179.8(3)	C7—C8—C9—C10	1.7(6)
C5—N1—C2—N3	0.2(3)	C8—C9—C10—C11	−1.7(6)
C2—N1—C5—C4	0.2(3)	C9—C10—C11—C6	0.9(6)
C27—N1—C2—N3	178.9(3)	C4—C12—C17—C16	177.4(3)
C27—N1—C2—C18	−1.1(5)	C4—C12—C13—C14	−177.0(4)
C27—N1—C5—C6	1.1(4)	C17—C12—C13—C14	0.0(6)
C2—N1—C27—C28	−85.7(4)	C13—C12—C17—C16	0.5(5)
C2—N1—C27—C32	96.2(4)	C12—C13—C14—C15	−0.7(7)
C5—N1—C27—C28	92.8(3)	C13—C14—C15—C16	1.0(7)
C5—N1—C27—C32	−85.4(3)	C14—C15—C16—C17	−0.6(7)
C2—N1—C5—C6	179.9(2)	C15—C16—C17—C12	−0.2(6)
C27—N1—C5—C4	−178.5(2)	C2—C18—C23—O24	1.7(4)
C2—N3—C4—C5	0.7(3)	C2—C18—C19—C20	178.3(3)
C2—N3—C4—C12	−178.6(3)	C23—C18—C19—C20	0.0(5)
C4—N3—C2—N1	−0.6(3)	C19—C18—C23—C22	0.6(4)
C4—N3—C2—C18	179.4(3)	C2—C18—C23—C22	−177.8(3)
N1—C2—C18—C19	0.1(5)	C19—C18—C23—O24	−179.8(3)
N3—C2—C18—C23	−1.7(4)	C18—C19—C20—C21	−0.2(6)
N1—C2—C18—C23	178.4(3)	C19—C20—C21—C22	−0.2(5)
N3—C2—C18—C19	−180.0(3)	C20—C21—C22—C23	0.8(5)
C12—C4—C5—N1	178.7(3)	C20—C21—C22—O25	−178.8(3)
C12—C4—C5—C6	−0.9(5)	O25—C22—C23—O24	−1.0(4)
N3—C4—C12—C13	−2.0(4)	O25—C22—C23—C18	178.6(3)
N3—C4—C12—C17	−178.8(3)	C21—C22—C23—O24	179.4(3)
C5—C4—C12—C13	178.8(3)	C21—C22—C23—C18	−1.0(4)
N3—C4—C5—N1	−0.6(3)	N1—C27—C28—C29	−179.5(3)
N3—C4—C5—C6	179.9(3)	C32—C27—C28—C29	−1.4(4)
C5—C4—C12—C17	2.0(5)	N1—C27—C32—C31	178.1(3)
C4—C5—C6—C7	90.5(4)	C28—C27—C32—C31	0.0(5)
C4—C5—C6—C11	−91.8(4)	C27—C28—C29—C30	1.2(5)
N1—C5—C6—C11	88.7(3)	C28—C29—C30—C31	0.4(5)
N1—C5—C6—C7	−89.0(3)	C28—C29—C30—C33	178.7(3)
C5—C6—C7—C8	177.9(3)	C29—C30—C31—C32	−1.8(6)
C7—C6—C11—C10	−0.1(5)	C33—C30—C31—C32	179.8(4)
C11—C6—C7—C8	0.1(4)	C30—C31—C32—C27	1.6(5)

Table 5. Hydrogen bond geometry (Å, °).

D—H···*A*	*D*—H	H···*A*	*D*···*A*	*D*—H···*A*
O24—H24···N3	0.82	1.82	2.560(3)	149
C13—H13···N3	0.93	2.55	2.882(4)	101
C28—H28···O24$^{(i)}$	0.93	2.56	3.335(4)	141

Symmetry code: (i) $x+1/2$, $-y+1/2$, $-z+1/4$.

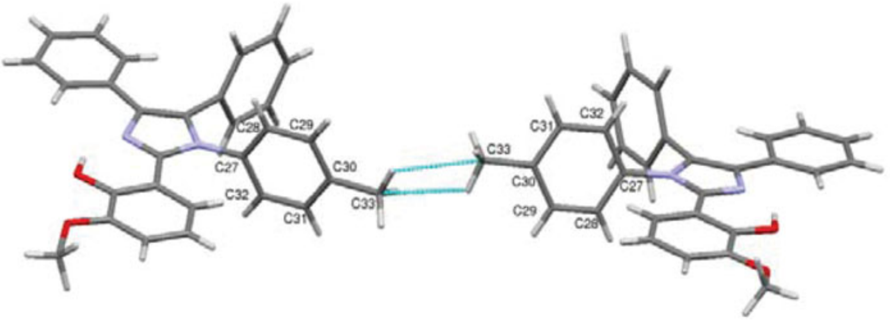

Figure 6. The bridging of molecules through R_2^2 (4) ring motif formed due to the interaction between methyl groups.

a six-membered planar ring C2/N3/H24/O24/C23/C18 fused with the imidazole ring. The crystal structure is further stabilized by C—H···O hydrogen bond interactions as listed in Table 5. The molecules are also connected through $R_2^2(4)$ ring motif's [17] formed due to the interaction between methyl groups as shown in Fig. 6.

3.6. Hirshfeld Surface Analysis

In order to visualize the intercontacts, Hirshfeld surface of the molecule was analyzed by the computational methods implemented in *CRYSTAL EXPLORER* [18]. The Hirshfeld

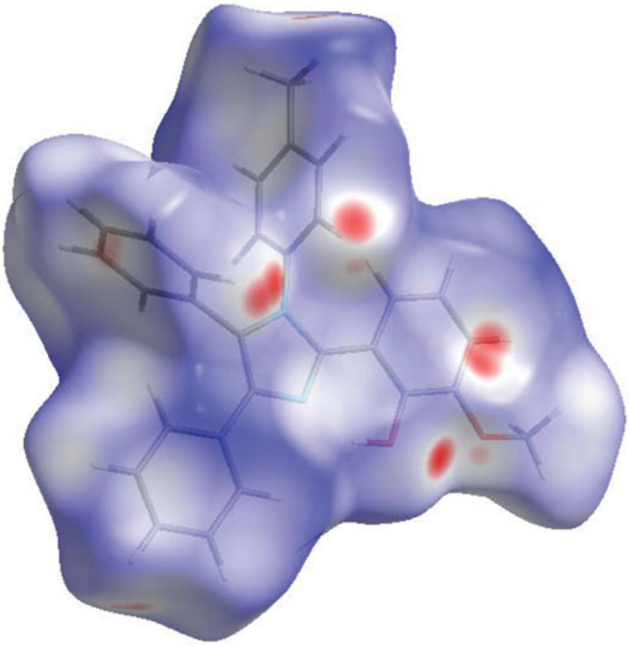

Figure 7. d_{norm} mapped on the Hirshfeld surface for visualizing the intercontacts of the molecule. Color scale between −0.050 au (blue) and 1.100 au (red).

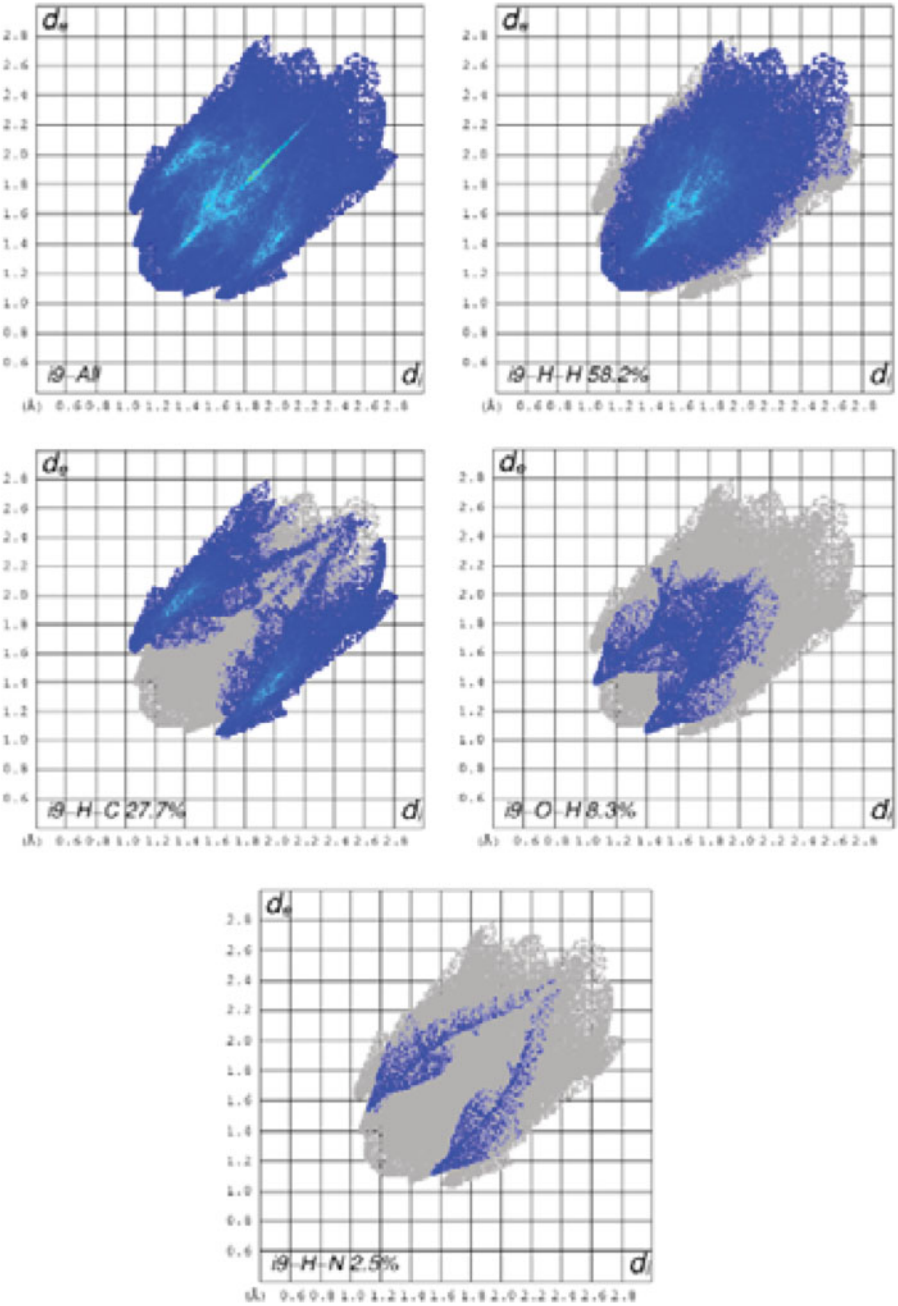

Figure 8. Fingerprint plots of the molecule.

surface and the fingerprint plots obtained due to the intercontacts between various atoms which are responsible for the formation of the Hirshfeld surface are shown in Figs. 7 and 8, respectively. The Hirshfeld surface analysis of the molecule proclaims that the dark spots occur on the surface as a result of hydrogen bond acceptors C28–H28···N3, O24–H24···N3, and C13–H13···N3 interactions.

It is evident from the fingerprint plots of the molecule that H···H (58%) intercontacts play a crucial role along with C···H (28%), O···H (8%), and N···H (2%) intercontacts for the formation of Hirshfeld surface, showing that these intercontacts are responsible for the stabilization of molecular and crystal structure.

4. Conclusion

Single crystal was grown by the slow evaporation method. The elemental analysis confirms the formation of the compound in a stoichiometric ratio. The UV-Vis spectrum reveals the properties of the crystals. The FTIR and proton NMR spectrum reveals the presence of the title compound, and TGA was carried out to study the thermal behavior of the crystal. The molecular structure of this compound was determined by single-crystal X-ray diffraction method. The molecular and crystal structures are stabilized by the C—H···N, O—H···N, and C—H···O hydrogen bond interactions.

Acknowledgments

The authors thank the Institution of Excellence, Vigyana Bhavan, University of Mysore, Mysore, Karnataka, India, for providing single-crystal X-ray diffraction facility to collect the data. The author VS gratefully acknowledge the UGC and DST-PURSE for the financial assistance and Mangalore University, USIC and MICROTONE center for their instrumental facilities. NMR research center Bangalore for the NMR spectrum.

References

[1] Wauquier, A., Van Den Broeck, W. A. E., Verheyen, J. L., & Janssen, P. A. J. (1978). *Eur. J. Pharmacol.*, *47*, 367.
[2] Tanigawara, Y., *et al.* (1999). *Clin. Pharmacol. Ther.*, *66*, 528.
[3] Heers, J., Backx, L. J. J., Mostmans, J. H., & VanCutsem, J. (1979). *J. Med. Chem.*, *22*, 1003.
[4] Cui, B., Zheng, B. L., He, K., & Zheng, Q. Y. (2003). *J. Nat. Prod.*, *66*(8), 1101.
[5] Satoru, I. (1989). *Chem. Abstr.*, *111*, 117, 867.
[6] Radziszewski, B. (1882). *Chem. Ber.*, *15*, 1493.
[7] Rideout, D. C., & Breslow, R. (1980). *J. Am. Chem. Soc.*, *102*(26), 7816.
[8] Prabhuswamy, M., Viveka, S., Madan Kumar, S., Nagaraja, G. K., & Lokanath, N. K. (2013). *Acta. Cryst.*, *E69*, o1006.
[9] Saberi, A., *et al.* (2009). *Mol. Cryst. Liq Cryst.*, *515*, 199.
[10] Gayathri, P., Thiruvalluvar, A., Srinivasan, N., Jayabharathi, J., & Butcher, R. J. (2010). *Acta. Cryst.*, *E66*, o2519.
[11] Bruker, (2012). *APEX2*, Bruker AXS Inc., Madison, Wisconsin, USA.
[12] Bruker, (2012). *SAINT PLUS*, Bruker AXS Inc., Madison, Wisconsin, USA.
[13] Sheldrick, G. M. (2008). *Acta. Cryst.*, *A64*, 112.
[14] Spek, A. L. (1990). *Acta. Crystallogr, Sect. A.*, *46*, C34.
[15] Macrae, C. F., *et al.* (2008). *J. Appl. Cryst.*, *41*, 466.
[16] Yanover, D., & Kaftory, M. (2009). *Acta. Cryst.*, *E65*, o711.
[17] Bernstein J., Davis R. E., Shimoni L., & Chang N. L. (1995). *Angew. Chem. Int. Ed. Engl.*, *34*, 1573.
[18] Wolff, S. K., *et al.* (2012). *CRYSTAL EXPLORER*, Version 3.1.